Cluster Abundance Cosmology: Impact of Halo Triaxiality and Orientation on SZ selection and WL mass bias

Mm Universe 06/25/25

Harshda Saxena, Jack Sayers, CHEX-MATE collaboration

Motivation - Mass calibration issues

- Masses based on HSE assumptions - inherently biased!
- WL masses are not dependent on dynamical state of cluster
- But they have deviations from average relations dominated by projection effects
- Cosmological simulations have shown DM halos as triaxial, with correlations between triaxiality and formation history

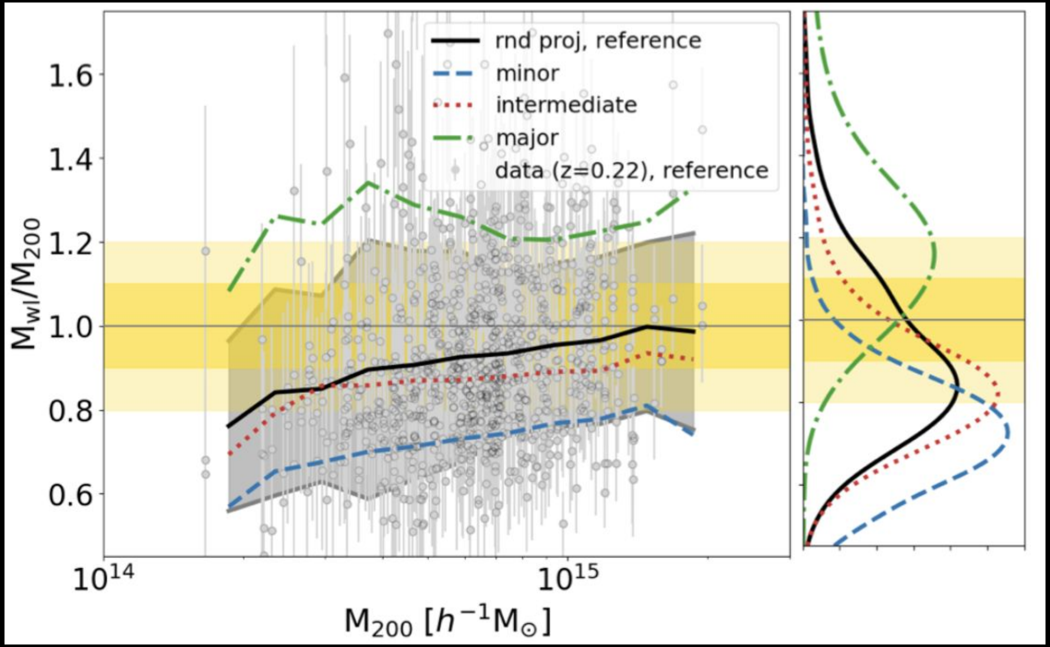

Euclid Collaboration 2024, WL masses using the 300 project hydrodynamical simulations

Research Goal

- Aim to answer -
  - Does survey selection based on observables like SZ effect result in a **biased detection population** of 3D triaxiality and orientation?
  - If yes, does this lead to a **WL mass bias**?

- Use the CHEX-MATE sample of clusters -
  - CHEX-MATE: The Cluster HEritage project with XMM-Newton - Mass Assembly and Thermodynamics at the Endpoint of structure formation
  - 3 Msec XMM-Heritage program
  - Planck SZ selected 118 clusters
  - Tier-1: volume-limited sample in the local universe

    $z < 0.2 \quad \text{and} \quad dec > 0$
  - Tier -2: sample of the most massive objects to have formed

    $z < 0.6 \quad \text{and} \quad M_{500} > 7.25 \times 10^{14}\, M_{sun}$
  - Have uniform and high-quality multi-wavelength data to fit for and quantify the 3D orientation

Cluster detection algorithm - Constructing MMF3

Characterize selection based on Planck's MMF3 algorithm - Used for the selection of the CHEX-MATE sample

Planck's cutout map $\boldsymbol{m}(\boldsymbol{x}) = y_0 \boldsymbol{t}_{\boldsymbol{\theta}_s}(\boldsymbol{x}) + \boldsymbol{n}(\boldsymbol{x})$

⬇

gNFW profile * Planck beam for model SZ emission map $\boldsymbol{t}_{\boldsymbol{\theta}_s}(\boldsymbol{x})_i$

⬇

Estimate the local noise as the cross-power spectrum $\boldsymbol{P}^{-1}(\boldsymbol{k})$

⬇

Construct the optimal filter $\boldsymbol{\Psi}_{\boldsymbol{\theta}_s}$

⬇

$$\mathrm{SNR} = \frac{\sum_x \boldsymbol{\Psi}_{\boldsymbol{\theta}_s}(\boldsymbol{x}) \boldsymbol{m}(\boldsymbol{x})}{\left[\sum_k \boldsymbol{t}_{\boldsymbol{\theta}_s}(\boldsymbol{k}) \boldsymbol{P}^{-1}(\boldsymbol{k}) \boldsymbol{t}_{\boldsymbol{\theta}_s}(\boldsymbol{k})\right]^{-1/2}}$$

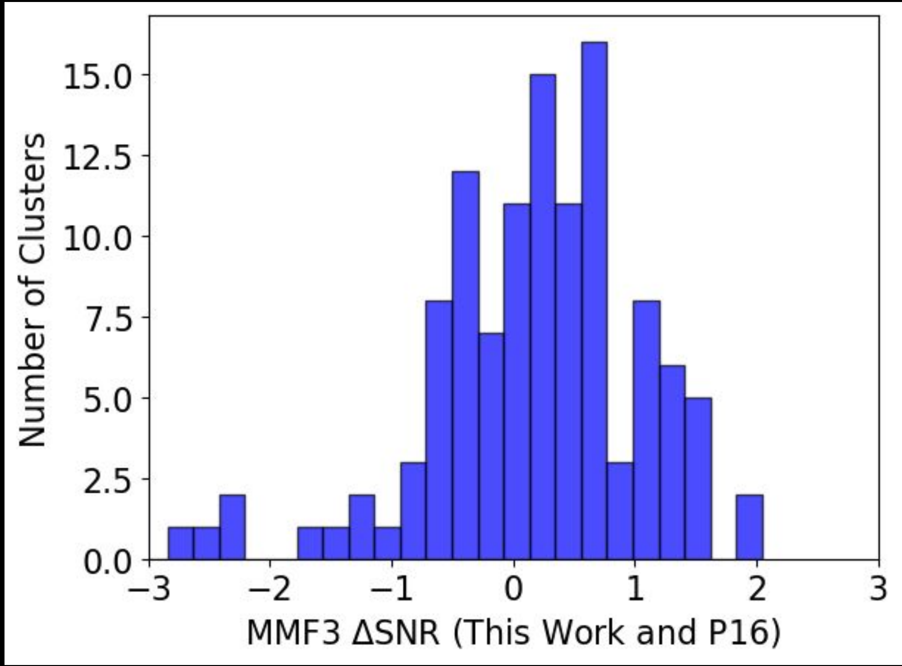

Saxena et al. 2025

Triaxial modelling

- Gas pressure profile: gNFW (Nagai et al. 2007; Arnaud et al. 2010)

$$\tau(x) = \frac{P_0}{(c_{500} * x)^{\gamma}[1 + (c_{500} * x)^{\alpha}]^{(\beta-\gamma)/\alpha}}$$

- Assume a geometry of a triaxial ellipsoid with the ICM pressure following gNFW described in this triaxial basis

- Assuming a triaxial ellipsoid shape, the projection of the 3D electron volume density onto plane of sky is done to understand the observables

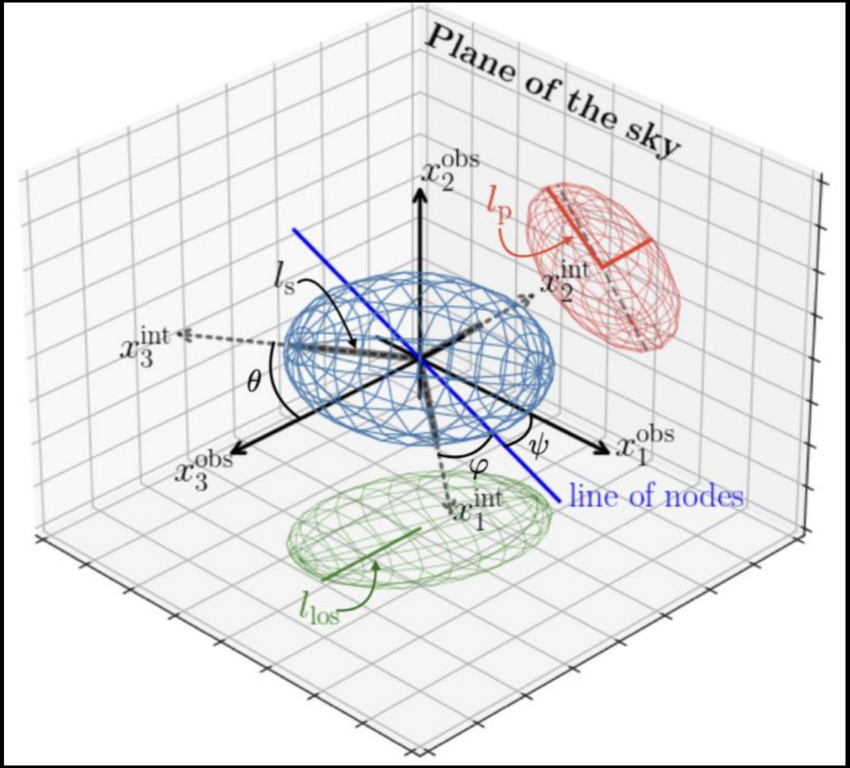

Kim et al 2024, CHEX-MATE: CLUster Multi-Probes in Three Dimensions (CLUMP-3D)

Triaxial Cluster completeness

Generate masks for the CHEX-MATE sample

⬇

Insert clusters of different SZ fluxes, cluster scales, triaxial ratios and orientations

⬇

Validate completeness pipeline for spherical clusters with Planck

⬇

Compute a lookup table with P(detection|SZ flux, cluster scale, triaxiality, orientation)

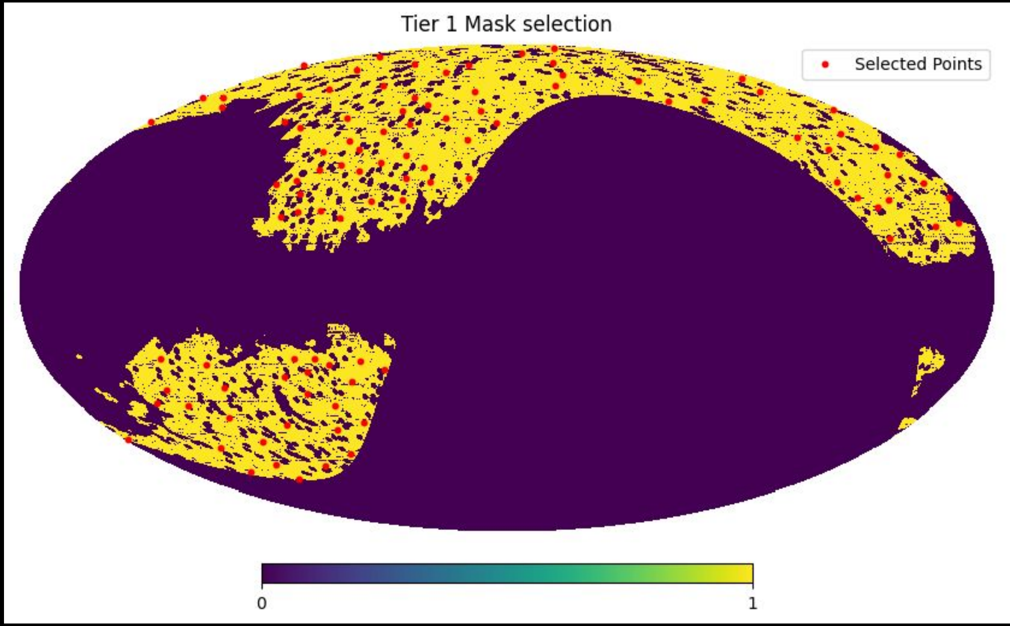

Triaxial Cluster completeness - contd.

Clusters along LOS have a higher probability of being detected

For different orientations, no trend between detectability and triaxiality

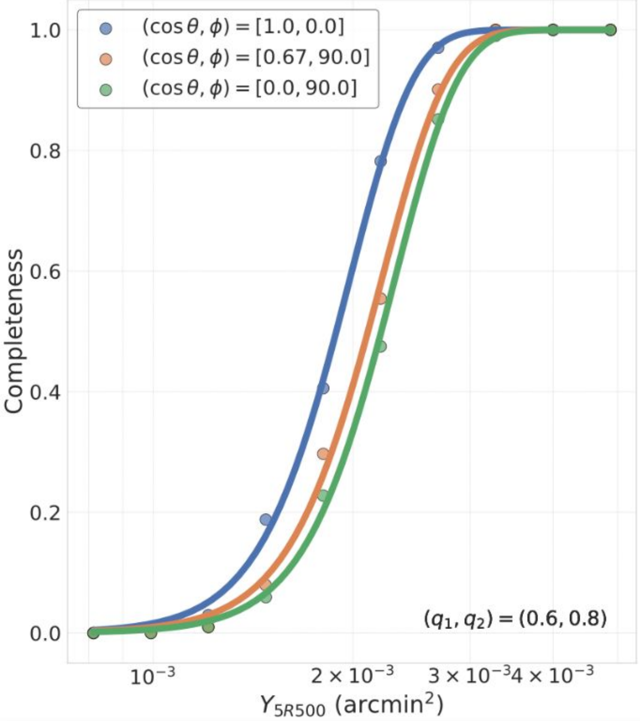

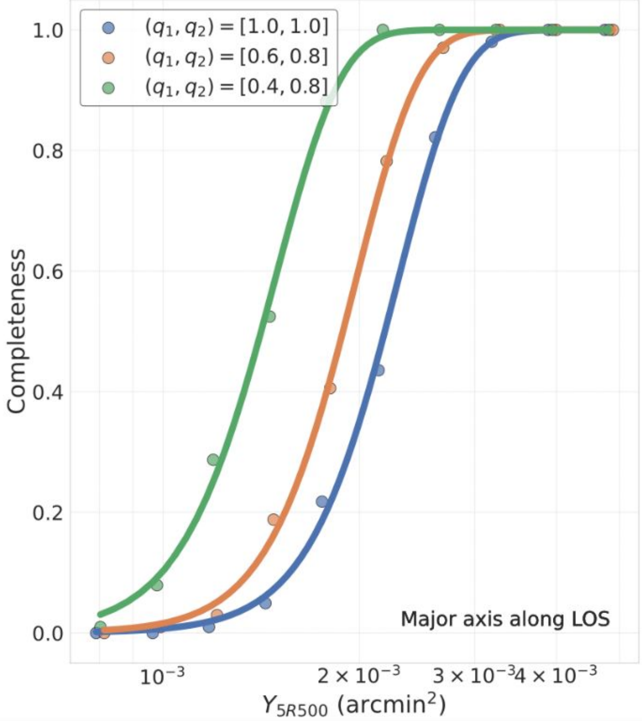

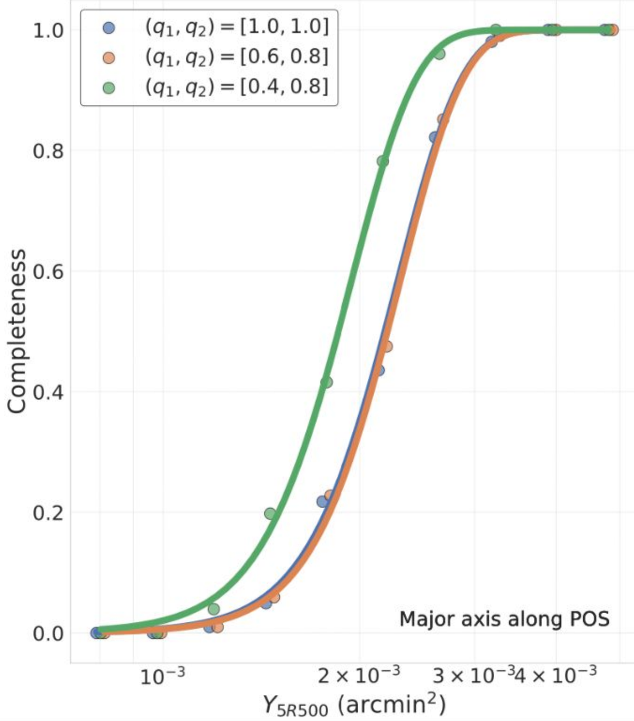

Saxena et al. 2025

Generating a mock catalogue

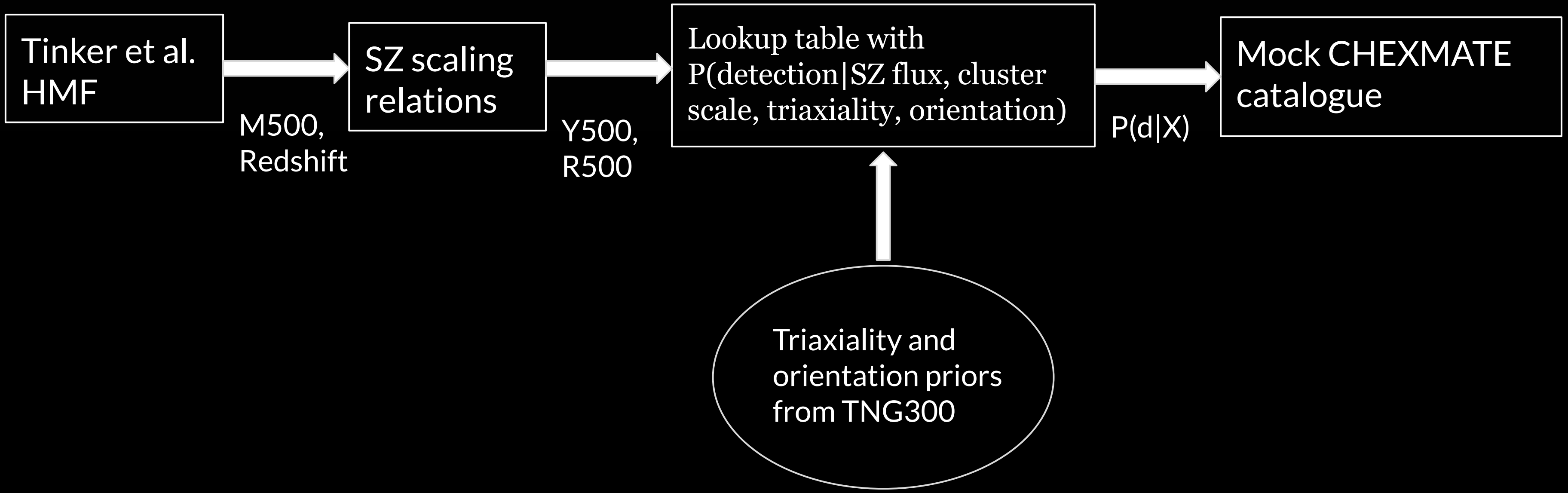

Mock catalogue results

- Bias in the detection for clusters to be oriented along the LOS - leads to a mass bias!

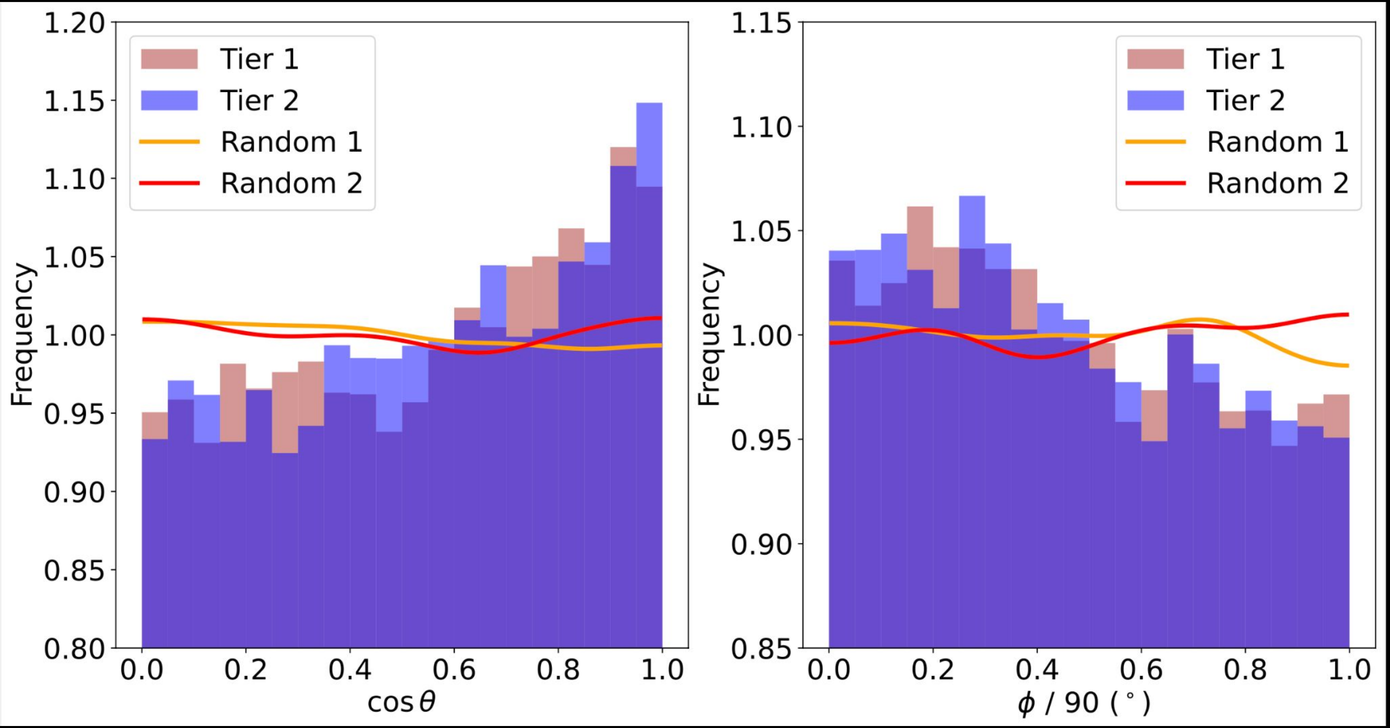

Saxena et al. 2025

Generating Mock Shear Maps

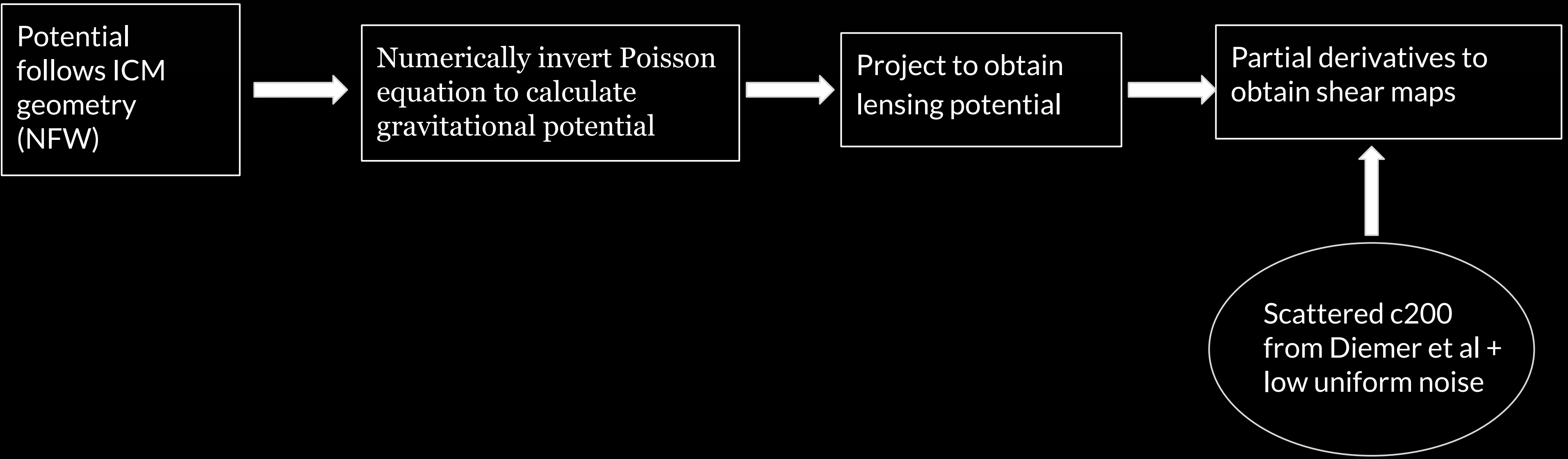

Weak lensing Mass fits

Fit - Spherically symmetric NFW model with Least Squares

Trend in boosted WL mass bias due to LOS orientation bias in selection at low masses

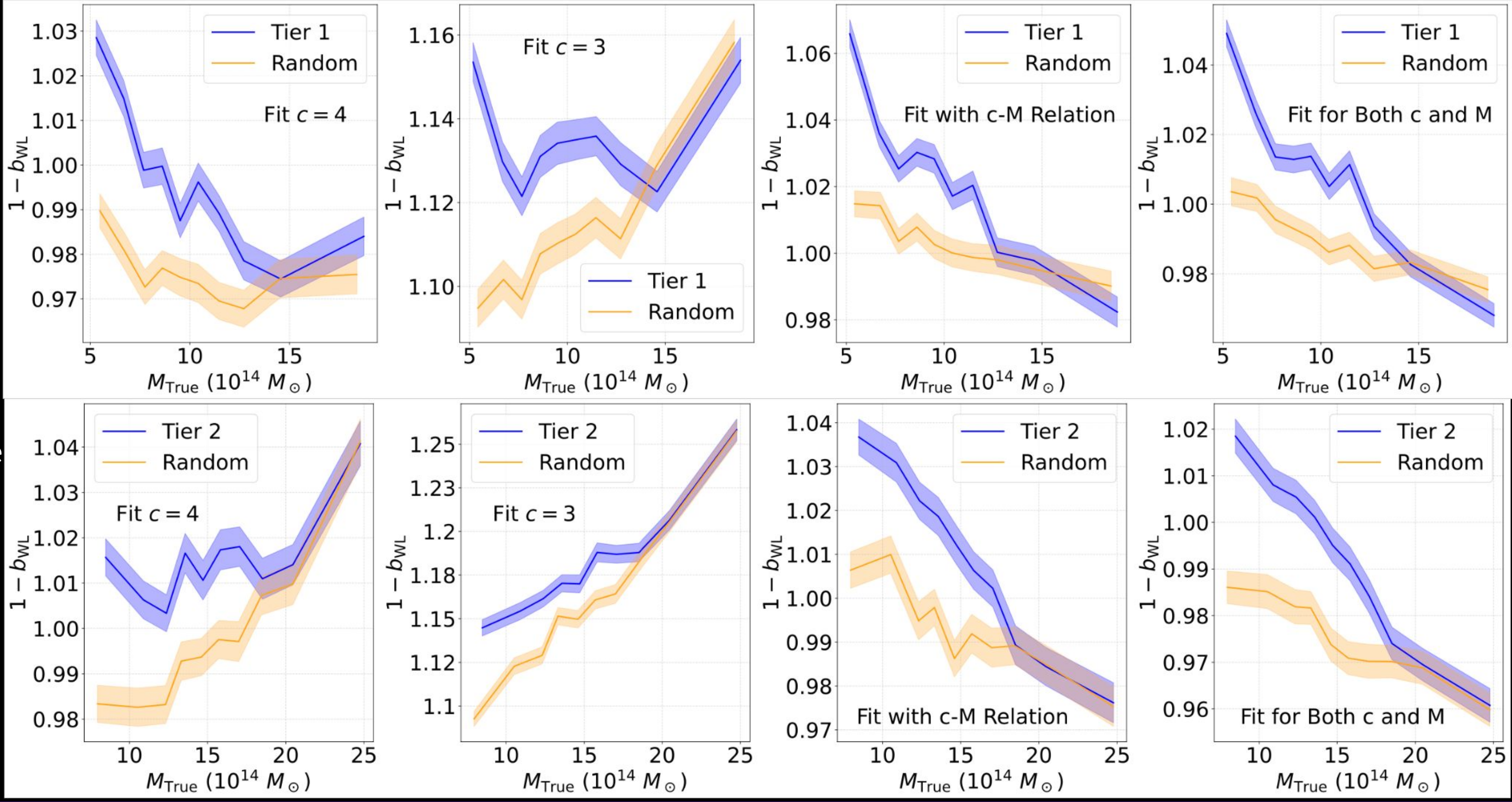

Saxena et al. 2025

Upscatter in WL mass bias due to selection

Ratio of WL mass bias of selected vs random sample independent of fitting!
Mass dependent bias due to selection, broken linear fit

CHEX-MATE	M_{break}	k
Tier 1	15.03×10^{14} $M_\odot$	−0.0039
Tier 2	21.67×10^{14} $M_\odot$	−0.0026

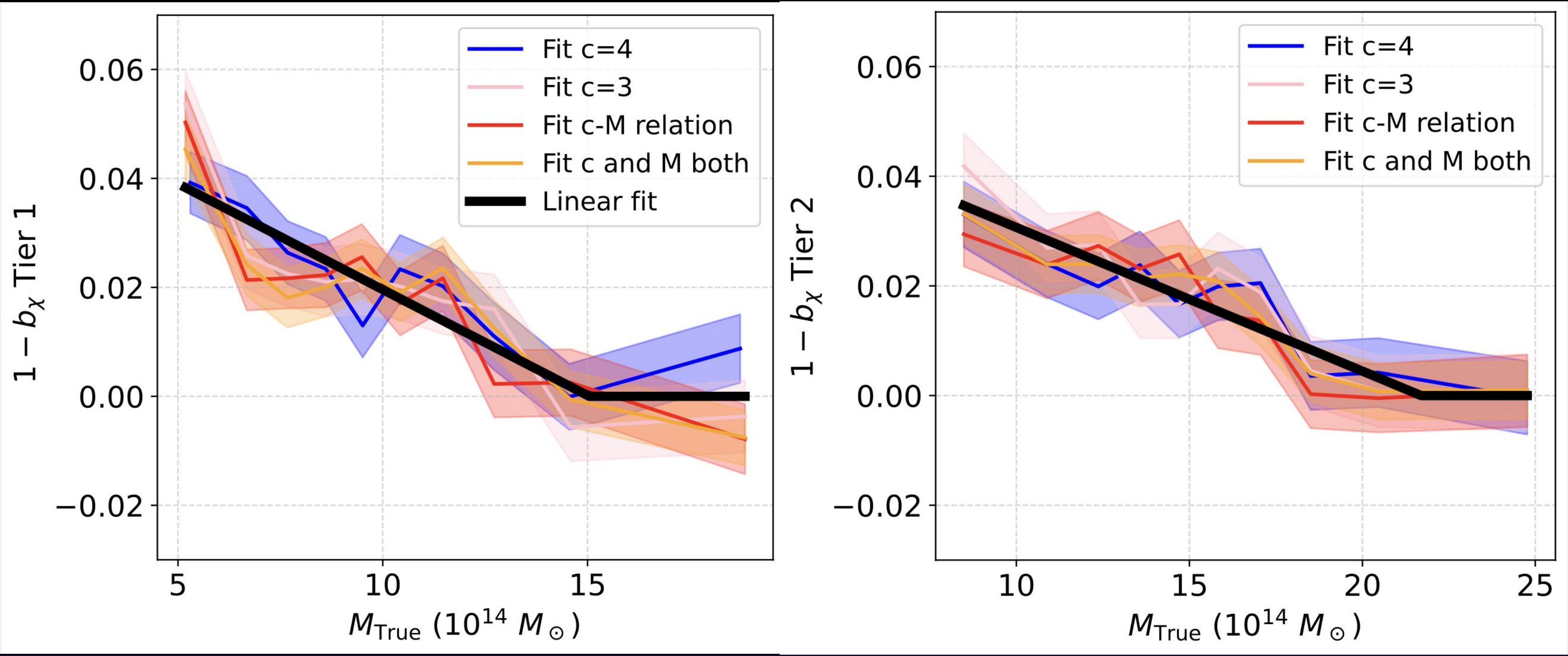

Saxena et al. 2025

Summary

- Constructed and validated the Multi-Matched Filtering (MMF3) algorithm against Planck for the detection and selection of clusters in all-sky SZ maps
- Built analytical triaxial cluster models to generate models of the mass distribution in clusters based on a elliptical generalization of the NFW profile
- Conducted MCMC injection and detection of mock clusters to calculate the completeness for a set of both spherical and triaxial clusters, and quantify the differences in completeness due to shape and orientation
- Generated a mock universe simulation of the CHEX-MATE sample, and performed the Tier 1 and Tier 2 selection including this shape and SZ flux dependent completeness
- Generated and fit mock shear maps to obtain the ratio of WL mass bias of selected vs random samples which is mass dependent and fitting methodology independent
- A new selection based WL mass bias - Needs to be taken account for SPT-3G, Euclid, etc

https://arxiv.org/abs/2505.23005

Backup Slides

Multi-wavelength information - tSZ effect

- Cool CMB photons IC scatter from hot ICM gas, leading to a spectral distortion in the CMB
- Observables are the SZ y-map, with instruments like Planck/SPT/ACT
- Surface Brightness of SZ effect is independent of redshift, making surveys mass-limited upto all redshifts
- Probe electron pressure - $y \equiv \frac{\sigma_T}{m_e c^2} \int_{\|} P_e dl = \frac{\sigma_T k_B}{m_e c^2} \int_{\|} n_e T_e dl,$

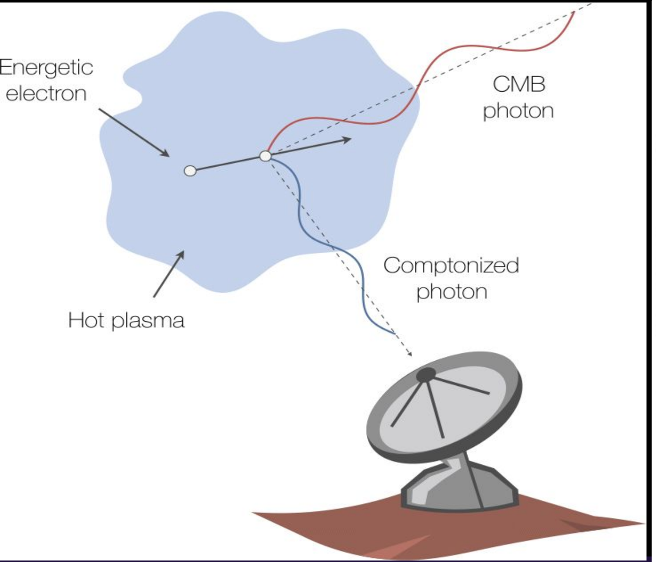

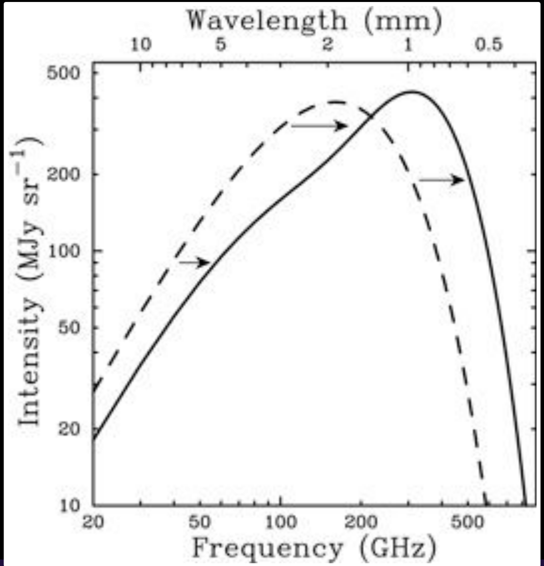

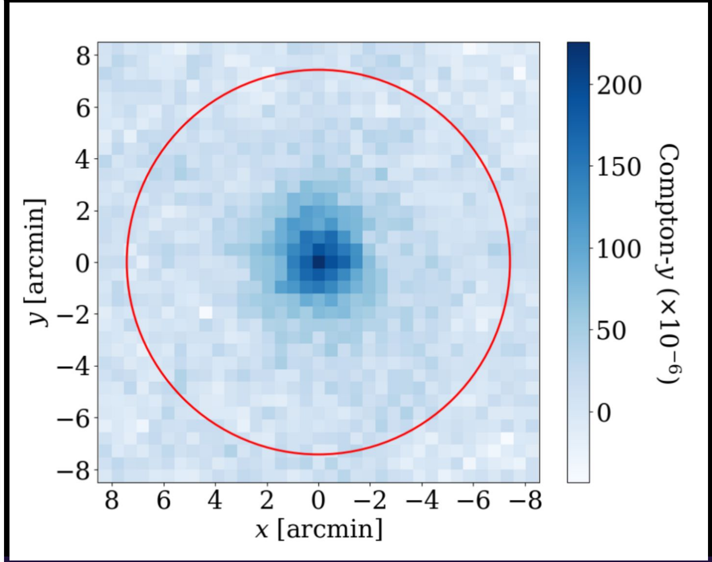

Planck's cutout map $m(x) = y_0 t_{\theta_s}(x) + n(x)$

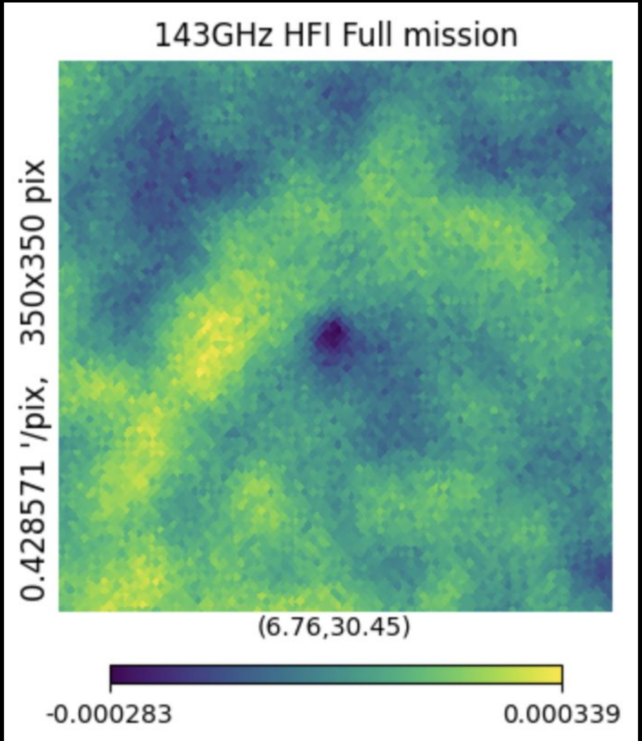

Convolve Planck's beams with the gNFW profile to generate a model SZ emission map $t_{\theta_s}(x)_i$

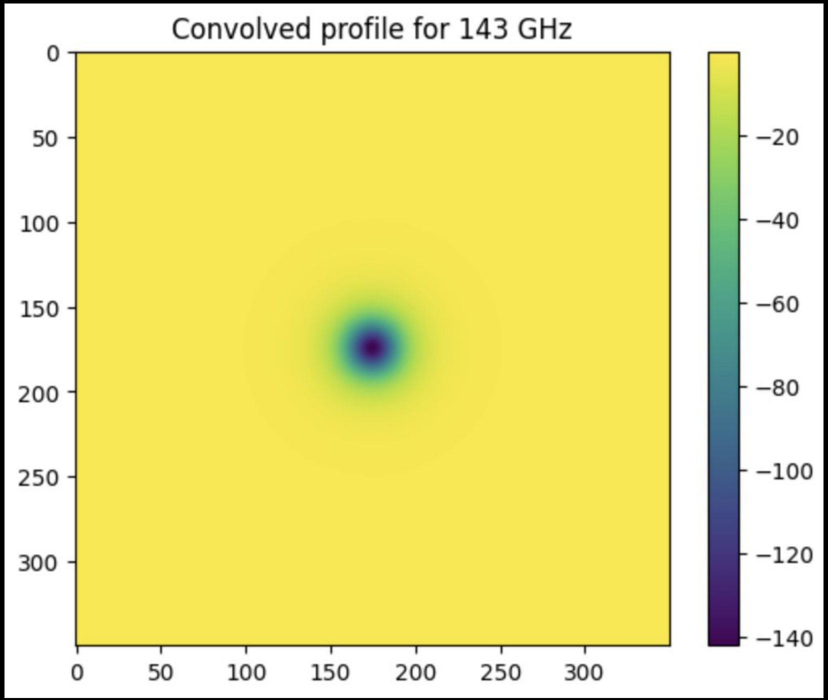

Constructing MMF3 - contd.

Estimate the local noise as the cross-power spectrum $\boldsymbol{P^{-1}(k)}$

Construct the optimal filter $\boldsymbol{\Psi_{\theta_s}}$

$$\mathrm{SNR} = \frac{\sum_x \boldsymbol{\Psi_{\theta_s}(x) m(x)}}{\left[\sum_k \boldsymbol{t_{\theta_s}(k) P^{-1}(k) t_{\theta_s}(k)}\right]^{-1/2}}$$

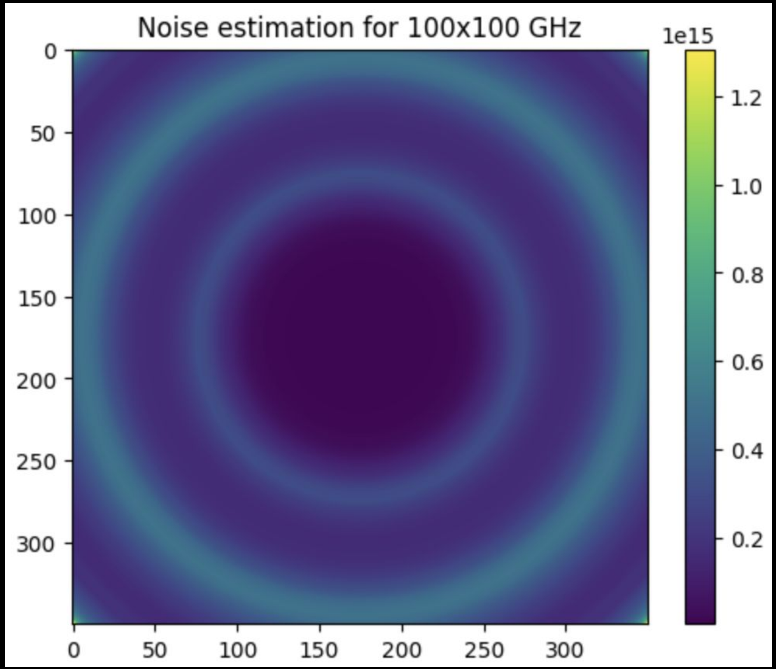

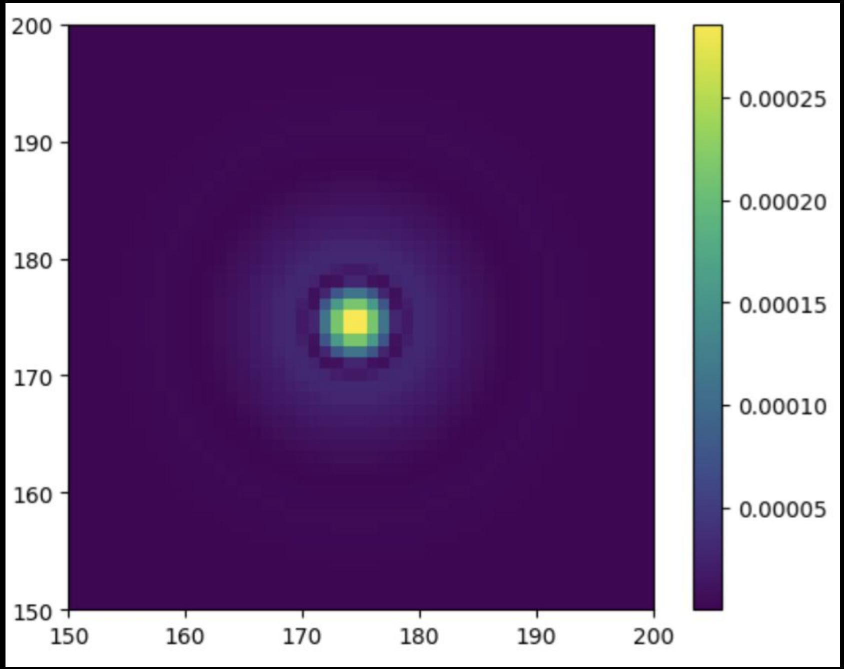

Compare SNR for CHEX-MATE clusters,
Std. dev = 0.7, factor of 2 lower than Planck's internal consistency between algorithms!

Compare the derived integrated flux: $Y_{5R500} = \hat{y}_0 \int_{\theta < 5\theta_{500}} \tau_{\theta_s}(r) dr$

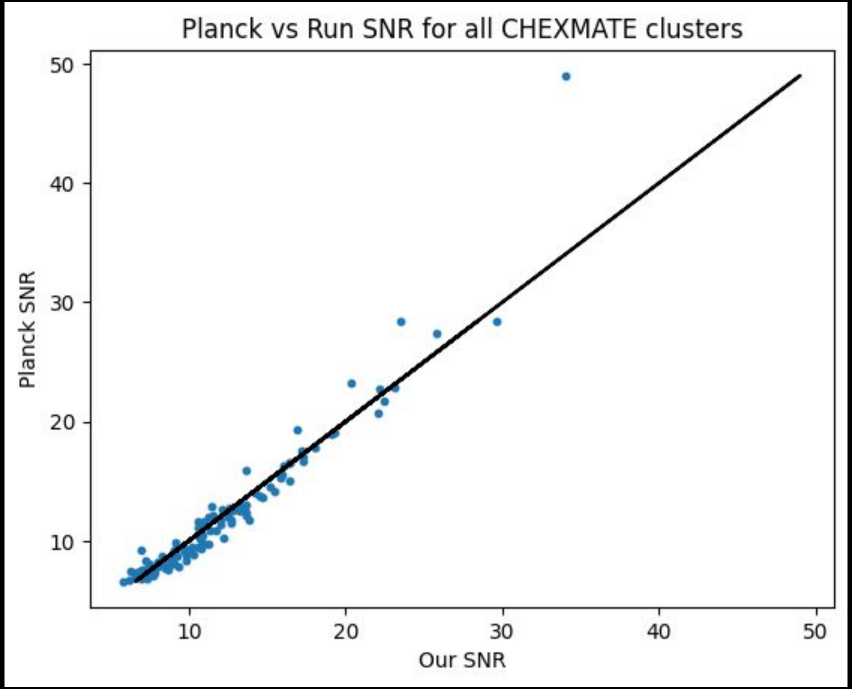

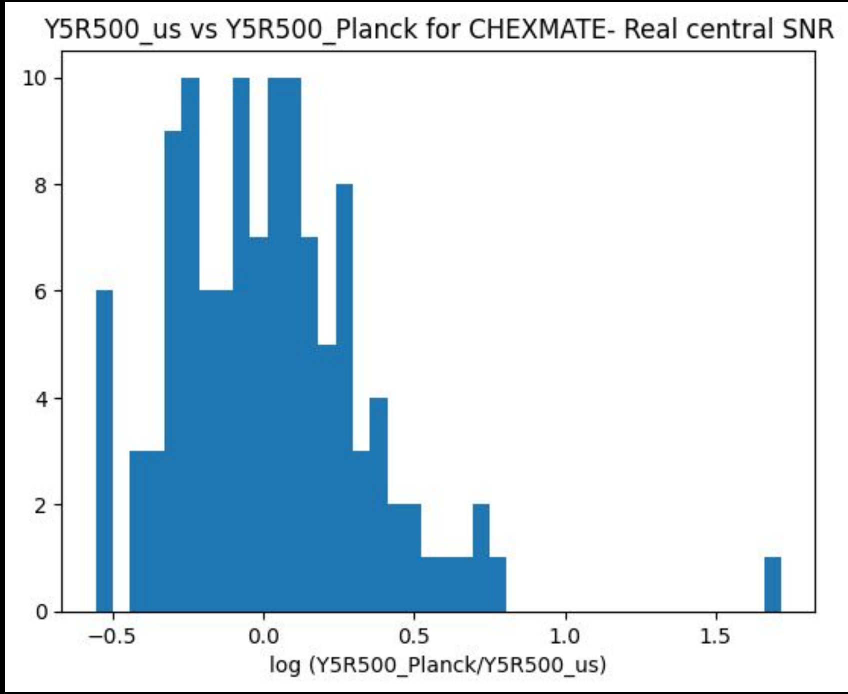

Significantly different fluxes due to orientations for triaxial ellipsoids!

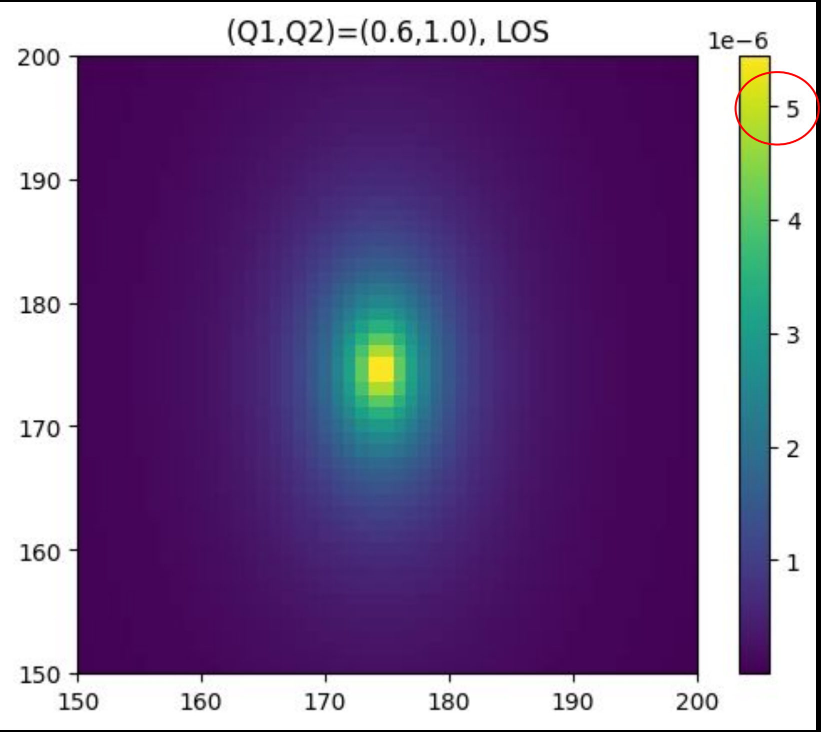

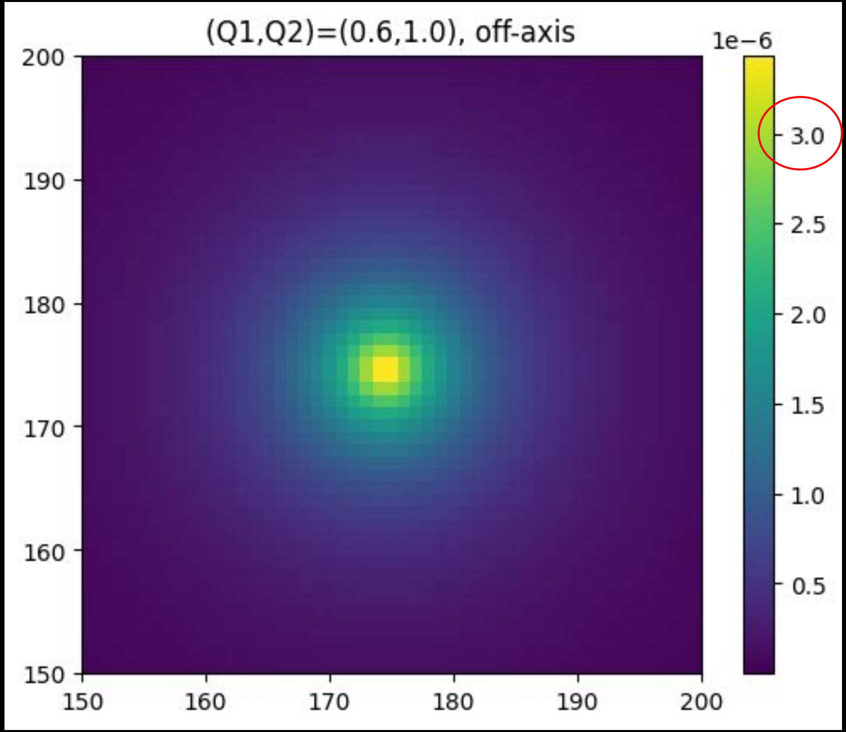

Insert mock clusters in unmasked regions

Insert clusters of different fluxes and scales, compute the probability of detection above some SNR threshold (completeness)

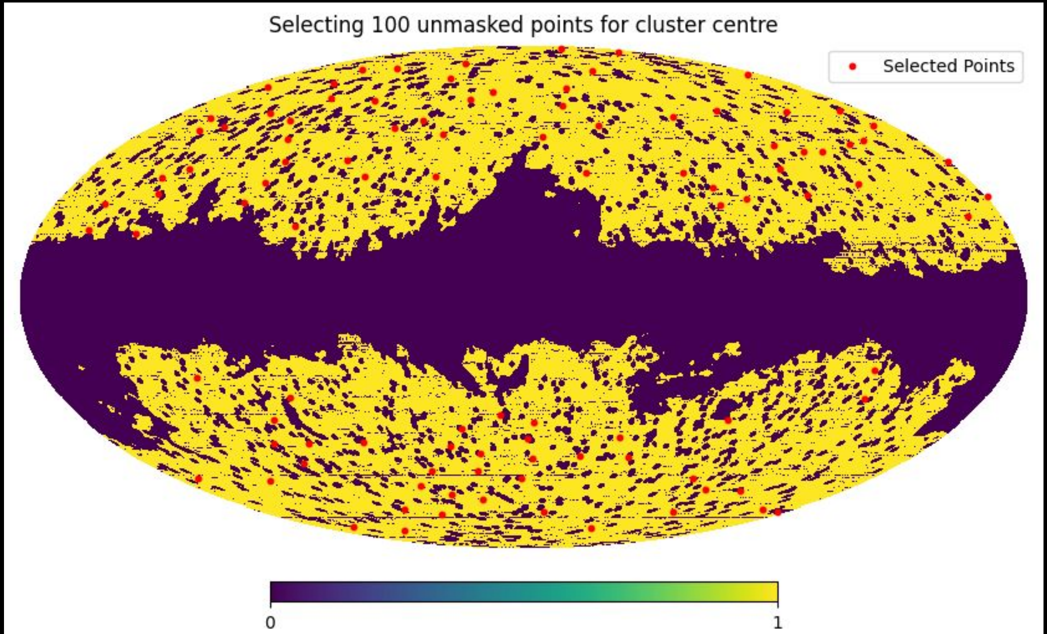

- Compare completeness with Planck
- Compare with an expected “semi-analytical” completeness

Percent-level agreements with semi-analytical completeness

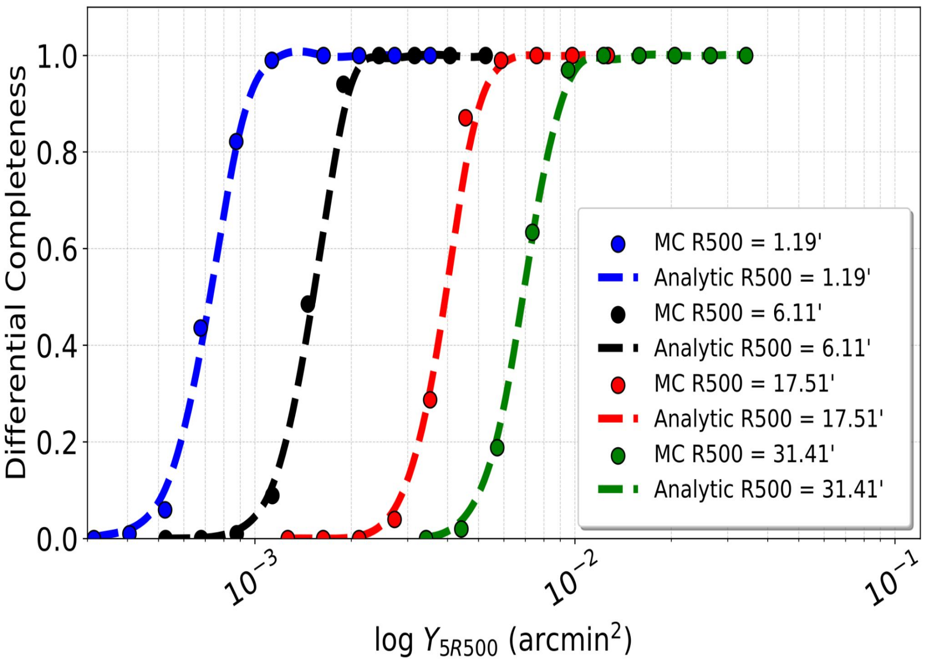

Planck's agreement with semi-analytical completeness

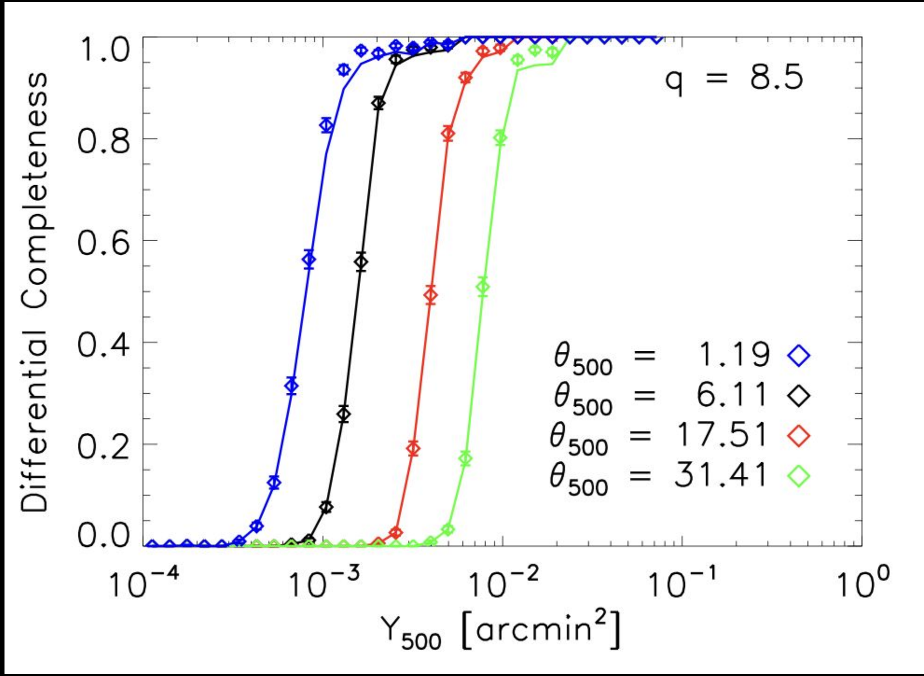

MMF3 details

- GNFW profile: $\tau(x) = \dfrac{P_0}{(c_{500} * x)^{\gamma}[1 + (c_{500} * x)^{\alpha}]^{(\beta-\gamma)/\alpha}}$ Convolved profile: $\boldsymbol{t}_{\boldsymbol{\theta_s}}(\boldsymbol{x})_i = j_\nu(\nu_i)[b_i * \tau_{\theta_s}](\boldsymbol{x})$
- With tSZ spectrum as: $j_\nu(\nu_i) = \nu_i T_{\mathrm{CMB}} \left[\dfrac{e^{\nu_i} + 1}{e^{\nu_i} - 1} - 4\right]$
- The noise is estimated directly from local maps, by first mean subtracting the maps, applying a Hanning window function, , computing the FFT of these maps, and then compute the cross-power spectra from these FFT's for the 6*6 channels, and azimuthally averaging, and then this cross-channel matrix is inverted for each pixel
- The Matched Multi-filter is the minimum variance estimate, and show Fourier ringing as a result of down-weighting the large angular scale modes contaminated with primary CMB and dust
- The HFI channels of Planck measure nearly identical dust emission. Thus, the covariance matrix is highly correlated between channels, resulting in a numerically unstable inversion for the calculation of the noise.

Triaxiality

- For the minor to major axial ratio of the projected ellipse - $q_{\mathrm{p}} = \sqrt{\frac{j+l-\sqrt{(j-l)^2+4k^2}}{j+l+\sqrt{(j-l)^2+4k^2}}}$

  Where j, k and l are complicated functions of the 3 Euler angles

- Projected length perpendicular to LOS is $l_{los} = l_s/\sqrt(f)$
- Semi-major axis of the projected ellipse - $l_{\mathrm{p}} = l_s\sqrt{\frac{q_1 q_2}{q_{\mathrm{p}}}} f^{1/4}$ $f = \sin^2\theta\left[\left(\frac{\sin\varphi}{q_1}\right)^2 + \left(\frac{\cos\varphi}{q_2}\right)^2\right] + \cos^2\theta$
- Elongation parameter of the ellipsoid - $e_{\parallel} \equiv \frac{l_{\mathrm{los}}}{l_{\mathrm{p}}} = \sqrt{\frac{q_{\mathrm{p}}}{q_1 q_2}} f^{-3/4}$
- Effective spherical radius on plane of sky- $l_{eff} = l_p(1-e_p^2)^{0.25}$
- Effective orientation parameter - $e'_{\Delta} = l_{eff}/l_{los}$

Effective orientation parameter with SNR

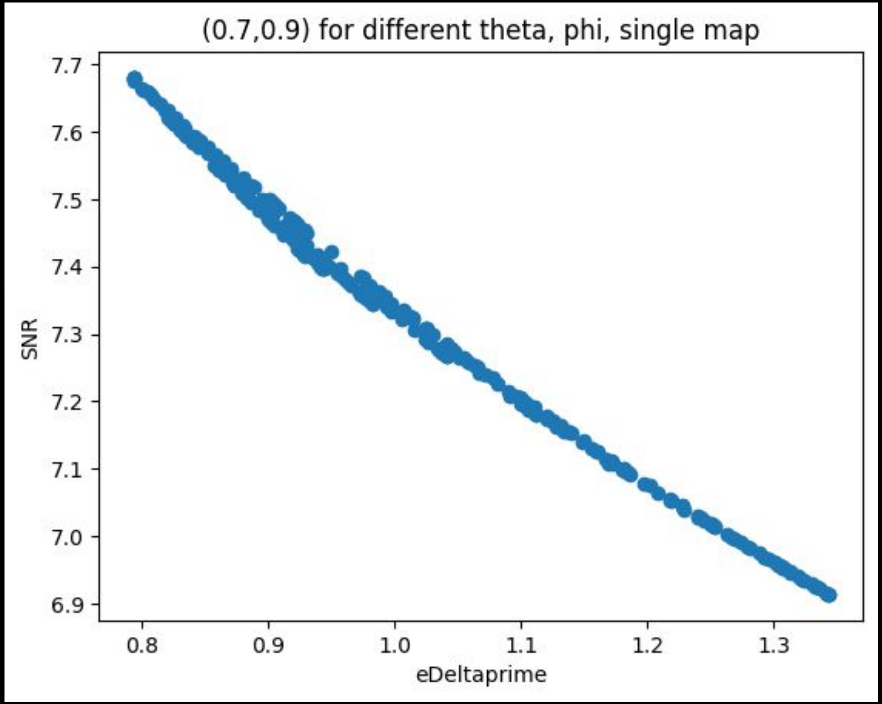

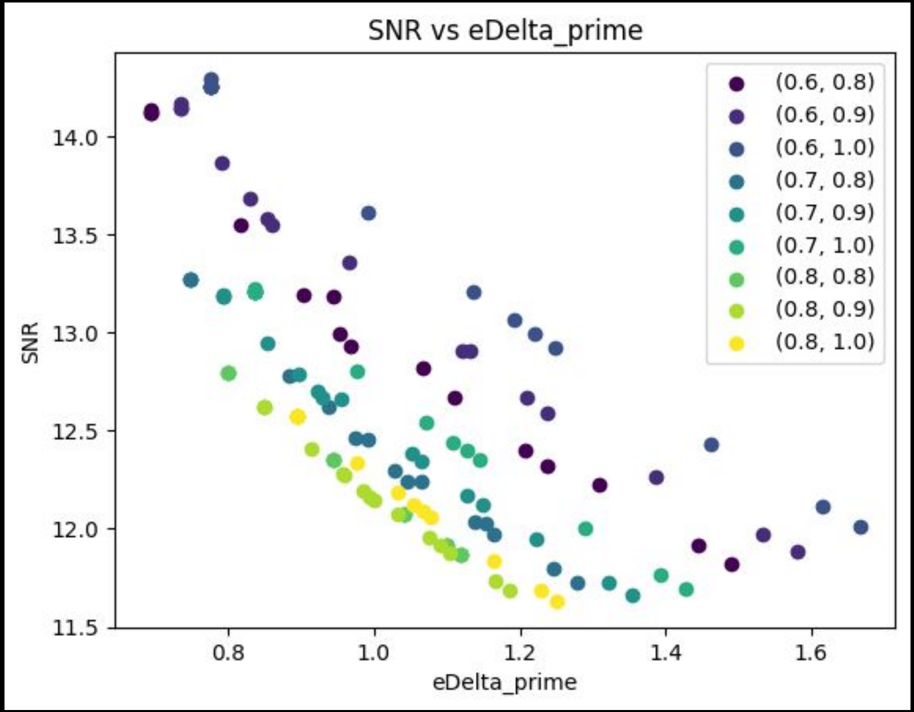

Interpolated a and b parameters

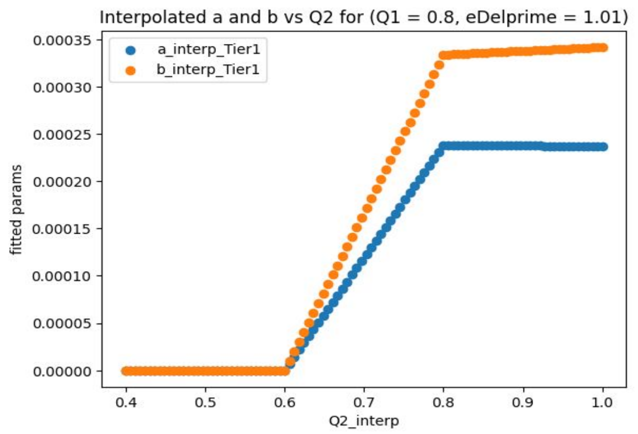

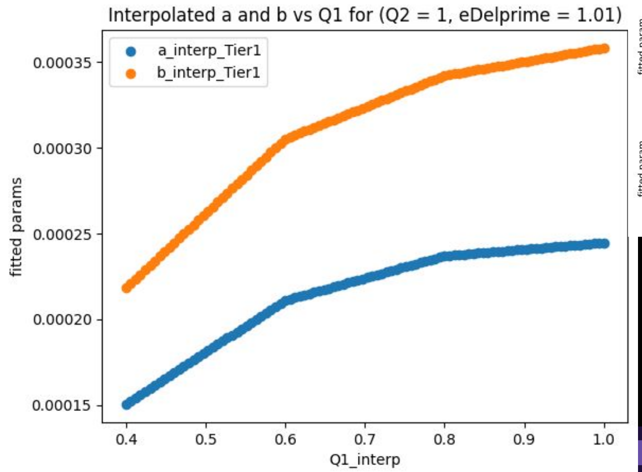

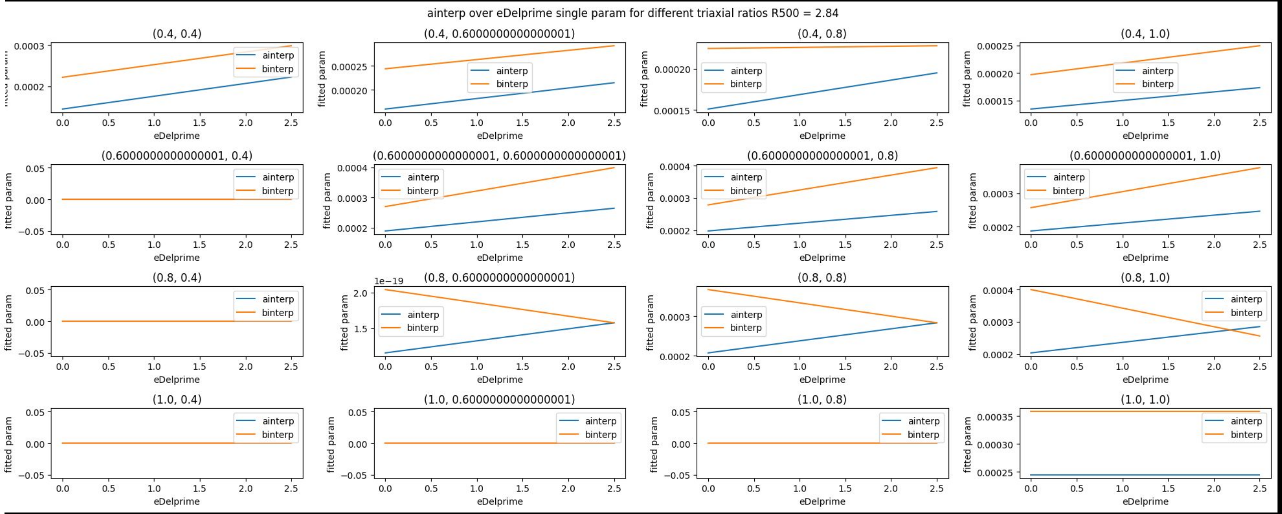

Q1-Q2 priors from Valle et. al

Left: More extreme triaxial shapes for gas predicted than for the data sent in simulations on the right

			$z = 0$			
		$r/r_{500} =$	0.1	0.5	1.0	2.0
All	DM	CSF	0.66 ± 0.05	0.47 ± 0.05	0.54 ± 0.04	0.39 ± 0.06
		NR	0.37 ± 0.03	0.38 ± 0.04	0.41 ± 0.05	0.28 ± 0.05
	Potential	CSF	0.59 ± 0.10	0.58 ± 0.08	0.55 ± 0.06	0.53 ± 0.05
		NR	0.49 ± 0.08	0.57 ± 0.07	0.56 ± 0.05	0.49 ± 0.05
	Gas	CSF	0.58 ± 0.05	0.67 ± 0.67	0.74 ± 0.04	0.70 ± 0.06
		NR	0.58 ± 0.05	0.65 ± 0.05	0.67 ± 0.06	0.63 ± 0.06
Relaxed	DM	CSF	0.76 ± 0.02	0.63 ± 0.05	0.67 ± 0.04	0.46 ± 0.10
		NR	0.41 ± 0.02	0.46 ± 0.06	0.48 ± 0.07	0.30 ± 0.10
	Potential	CSF	0.91 ± 0.01	0.82 ± 0.02	0.71 ± 0.02	0.65 ± 0.03
		NR	0.65 ± 0.03	0.72 ± 0.06	0.67 ± 0.05	0.58 ± 0.02
	Gas	CSF	0.61 ± 0.07	0.79 ± 0.05	0.80 ± 0.03	0.82 ± 0.02
		NR	0.61 ± 0.07	0.74 ± 0.03	0.76 ± 0.02	0.72 ± 0.05

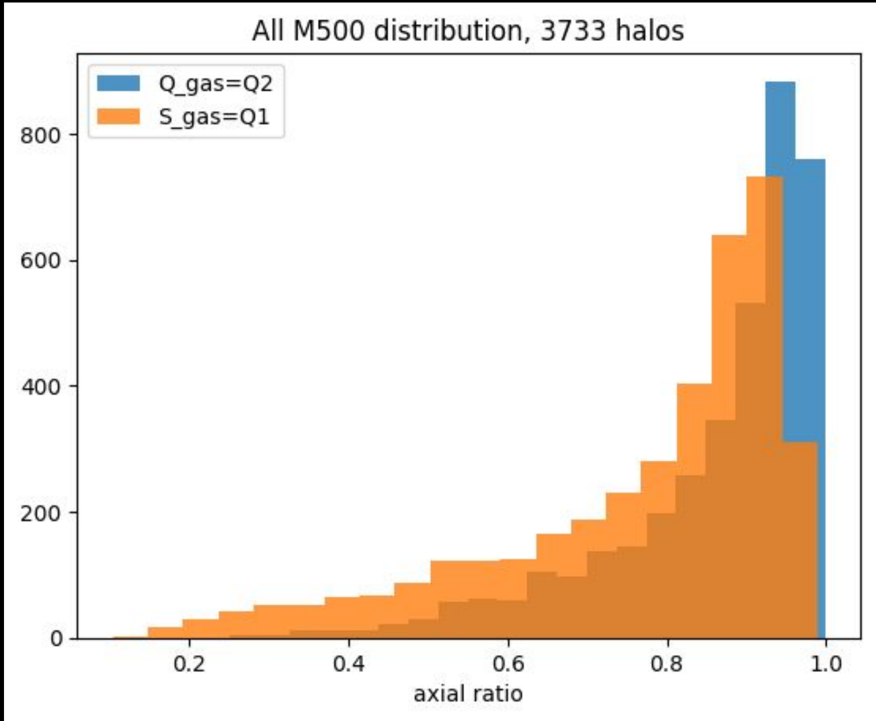

Generating a mock catalogue

- Use the Tinker et al. HMF to generate the N(M,z) within the sky fractions for both Tier 1 and Tier 2
- Convert to SZ parameters using the scaling relations -

$$\bar{\theta}_{500} = \theta_* \left[\frac{h}{0.7}\right]^{-2/3} \left[\frac{(1-b)M_{500}}{3 \times 10^{14} \mathrm{M}_\odot}\right]^{1/3} E^{-2/3}(z) \left[\frac{D_\mathrm{A}(z)}{500 \mathrm{Mpc}}\right]^{-1}$$

$$E^{-\beta}(z) \left[\frac{D_\mathrm{A}^2(z)\bar{Y}_{500}}{10^{-4} \mathrm{Mpc}^2}\right] = Y_* \left[\frac{h}{0.7}\right]^{-2+\alpha} \left[\frac{(1-b)M_{500}}{6 \times 10^{14} \mathrm{M}_\odot}\right]^{\alpha}$$

- Use TNG300 simulations from Valle et al. to quantify Q1 and Q2 priors, and set uniform priors for the two angles
- Use the lookup table to compute the completeness for each halo, and select it on a random draw into our detected catalogue, quantify the orientation bias of the detected vs all clusters

Tier 1 Histograms

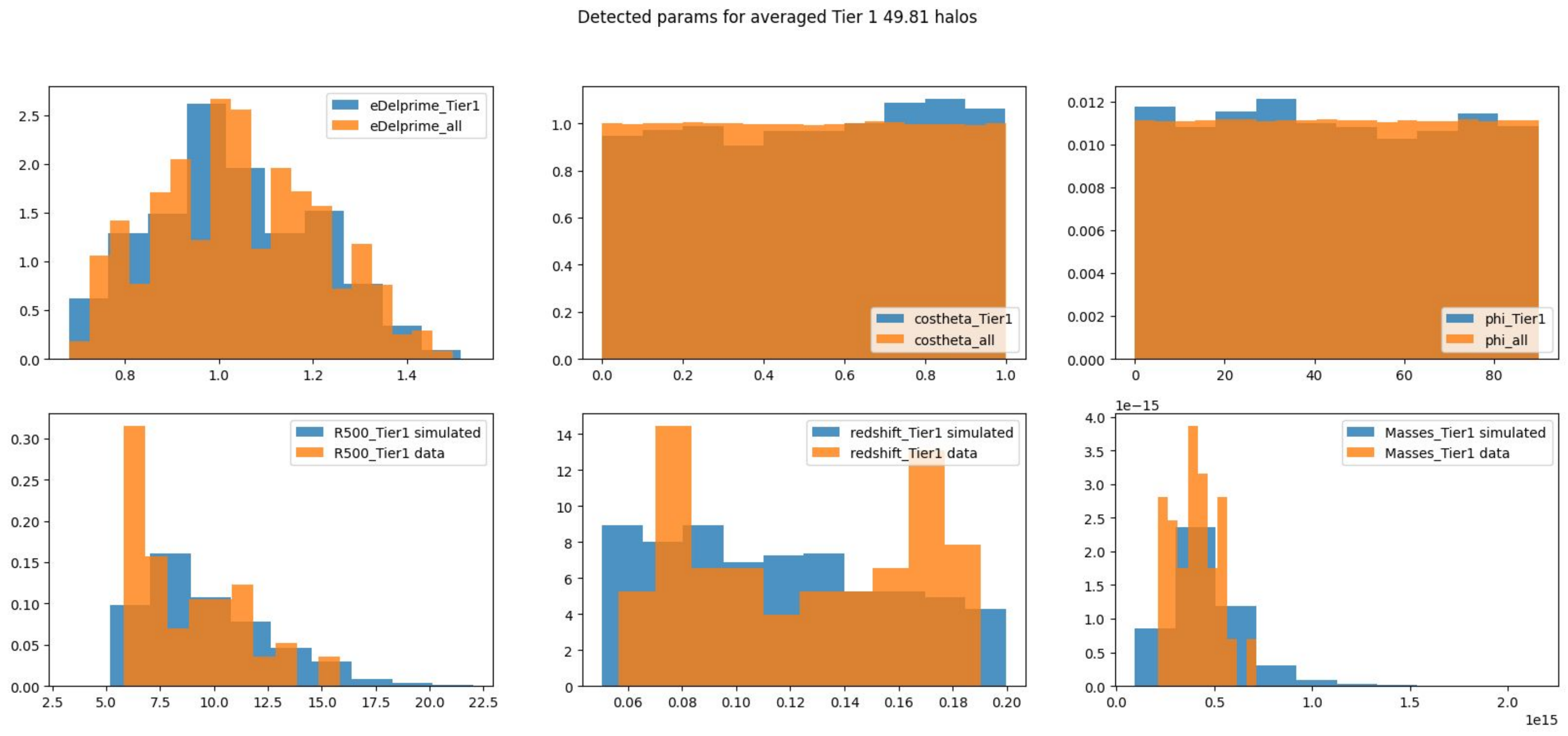

More extreme triaxial priors